ACS APPLIED MATERIALS & INTERFACES

Research Article

www.acsami.org

Preparation of Self Assembled Sodium Oleate Monolayer on Mild Steel and Its Corrosion Inhibition Behavior in Saline water

H. N. Shubha,[†] T. V. Venkatesha,*[,†] K. Vathsala,[‡] M. K. Pavitra,[†] and M. K. Punith Kumar[§]

[†]Department of Studies in Chemistry, School of Chemical Sciences, Kuvempu University, Shankaraghatta 577451, Karnataka, India

[‡]Department of Chemical Engineering, Tuskegee University, Tuskegee, Alabama 36088, United States

[§]Department of Materials Engineering, Indian Institute of Science, Bangalore 560 012, Karnataka, India

ABSTRACT: A self assembled monolayer (SAM) of sodium oleate was generated on mild steel by the dip coating method. Formation of the SAM on mild steel was examined using Infrared Reflection Absorption Spectroscopy (IRRAS) and contact angle measurements. The chemical and anticorrosive properties of the SAM were analyzed using different techniques. IRRAS and water contact angle data revealed the crystallinity and chemical stability of the SAM modified mild steel. The electrochemical measurements showed that the mild steel with the sodium oleate derived SAM exhibited better corrosion resistance in saline water. The effect of temperature and pH on the SAM formation and its anti corrosion ability was explored.

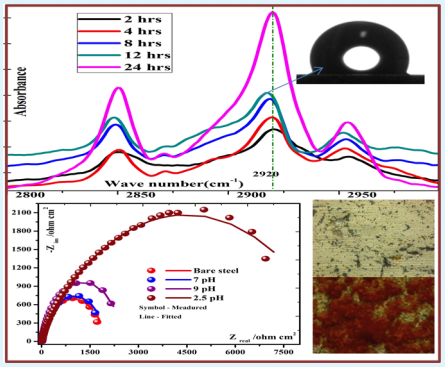

KEYWORDS: *self assembled monolayer, sodium oleate, contact angle, IRRAS, corrosion, EIS*

1. INTRODUCTION

Spontaneous formation of layer molecular assemblies of a surfactant on a substrate is generally referred to as a self assembled monolayer (SAM). The surfactant molecules adsorb on a substrate because of the specific affinity of their head groups and thus favor formation of mono molecular ordered layers.[1−4] When SAM is formed the head group is in contact with the surface of the substrate and the tail group is free in space. The molecular backbones of different tails and their van der Waals interaction play an important role on the stability of SAMs.[5] Since the delicate balance of several interactions of different origin determines the behavior of SAMs, various models and approximation have been used to develop a sensible theoretical treatment, focusing on different aspects like head group bonding structure or the thermal behavior of the chains.[6]

SAMs have been utilized in many diverse technical applications: They are used as protective coatings;[7] the control of wetting property was the first and foremost application of organic monolayers;[8] friction and lubrication problems can be improved and modified by choosing a suitable end group.[9] SAMs are attractive for electrochemical applications like Sensors. SAMs were found to be ideal for biological applications since they create links between the organic and inorganic matter. The commonly studied monolayers include: thiols,[10,11] disulfides,[12,13] alkyl trichlorosilane,[14,15] fatty acids,[16,17] and alkyl phosphonates.[18,19]

SAMs can be characterized by a number of experimental methods which include physical measurements like contact angle,[20] spectroscopic techniques such as ellipsometry,[21] X-ray photon spectroscopy (XPS),[22] infrared spectroscopy (IR),[23] quartz crystalline membrane (QCM),[24] Surface enhanced Raman spectroscopy,[25] atomic force microscopy (AFM),[26] Scanning Tunneling microscopy,[27] and so forth.

Adsorption characteristics of oleic acid and its salts have been widely studied using several methods since they possess great surface activity. Adsorption of sodium oleate on an oxidized aluminum surface was studied by Rozenfel'd et al.[7] Luo et al. reported the corrosion inhibition of mild steel by sodium oleate in acidic solutions.[28] Vathsala et al. established the tribological property of the emulsion containing oleate molecule on a steel surface.[9] Xu et al. reported the effect of sodium oleate adsorption on the colloidal stability and zeta potential of detonation synthesized diamond particles in aqueous solutions.[29] The interaction force between an oil film and a steel substrate in water in presence of dispersed sodium oleate in oil was established by Kumar and Biswas.[30]

In this paper, we report the preparation of a sodium oleate SAM on mild steel by the dip coating method. The chemical and anticorrosive properties of the SAMs prepared on the mild steel were characterized using IRRAS, contact angle measurements, 3D optical profilometry and electrochemical measurements.

Received: July 19, 2013
Accepted: October 21, 2013
Published: October 21, 2013

2. EXPERIMENTAL SECTION

Materials and Sample Preparation. The experiments were carried out using mild steel samples of composition 0.04%C, 0.35% Mn, 0.022%P, 0.036%S, and remaining Fe. The mild steel samples of dimension 1 cm^2 area (exposed) were used for the electrochemical corrosion experiments. These samples were polished mechanically by using different grades of emery paper (220, 600, 1000, 2000, 2500) and then further sonicated with acetone and alcohol for 15 min to remove all polishing debris and then again sonicated with Millipore water for 20 min. These samples were flushed with a stream of dry nitrogen gas and were kept in an ultraviolet cleaning chamber (Bioforce, Nanosciences, U.S.) for 30 min to burn all carbonaceous contaminants. The test samples prepared as above were dipped in a freshly prepared sodium oleate solution(1 mM) at desired pH (pH 2.5, pH 7, pH 9) for different time (2 h to 24 h), taken out, rinsed and washed with ethanol (to remove physisorbed molecules) followed by *n*-hexane. Sodium oleate (Rolex Laboratory Reagent, Bombay, India) was used as received. Millipore purification (Milli-Q, U.S.A.) system was used to process distilled water to get deionized water. The aggressive solution of 3.5%NaCl (neutral sea water contains the same chlorine concentration.[31]) (Final Chemical Limited, Ahmadabad, India) was prepared by using Milli-Q water.

IRRAS Analysis. An infrared reflection absorption spectroscopy (IRRAS) (GX spectrometer, Perkin Elmer, U.S.A.) instrument outfitted with a liquid nitrogen cooled mercury cadmium telluride (MCT) detector was used to take the spectra. Before starting the experiments the sample and detector chambers were purged using nitrogen gas. All IR spectra reported here are referenced to bare steel substrate over 1024 optimized scans at 4 cm^{-1} resolution by using a p-polarized beam. A heating accessory (Harrick scientific corporation, New York, U.S.A.) was used for heating the samples up to 120 °C for 1 h. The spectral analysis was carried out using spectrum 3.02 version software (Perkin-Elmer, U.S.A.).

Contact Angle Measurement. An OCA 30 from DataPhysics Instruments GmbH, Germany was used to measure the contact angles. An automatic injection pump was used to reside droplets on a substrate for analysis. The contact angle of water on the sample was measured by the sessile drop method. All experiments were carried out at 296 K. Images of the Air/Liquid/Solid (A/L/S) systems were captured and processed using the 32-bit SCA 20 software. For the A/L/S system, the sample was kept in air (ambient phase) and then water droplets of 2 μL were placed on the sample from a syringe at slow rate.

Electrochemical Measurements. Electrochemical measurements were performed in a conventional three electrode glass cell using CHI660C electrochemical workstation (U.S.A. make) and were carried out at 300 K. A steel specimen, a platinum wire, and a saturated calomel electrode (SCE) were used as working, auxiliary, and reference electrodes, respectively.

The corrosion measurement test samples were positioned in a Teflon sample holder and the surface area open to the corrosive medium was 1 cm^2. To begin with, the sample was immersed in a 3.5% NaCl solution to establish the open circuit potential (E_{OCP}) or steady-state potential. The polarization measurements were carried out at a scan rate of 1 mV s^{-1}. The electrochemical impedance measurements were carried at OCP in the frequency range 1 mHz to 100 kHz with 5 mV sine wave as the excitation signal. Impedance data were analyzed using ZSimp-Win 3.21 software.

Surface Morphology. To visualize the surface of metal, a Zeta-20 True Color 3D Optical Profiler (Zeta Instruments, CA, U.S.A.) was used. After the experiment the metal samples were kept in a vacuum desiccator and were mounted on sample holder under the objective of the Optical Profiler, and the 2D photos were taken from the 50× magnified surface.

3. RESULT AND DISCUSSION

Characterization of SAM. The formation of SAM and its characterization was made by IR Spectroscopy. Figure 1a represents the SAM generated at different time intervals at pH 7 and Figure 1b shows the effect of temperature on the generated SAM. The FTIR Spectrum of the SAM recorded in the range 2800 to 3000 cm^{-1} shows three well resolved peaks. In each spectrum the peaks signify stretching vibrations of the asymmetric CH_3 stretch at 2960 cm^{-1}, the asymmetric CH_2 stretch at 2920 cm^{-1}, and the symmetric CH_2 stretch at 2850 cm^{-1}.

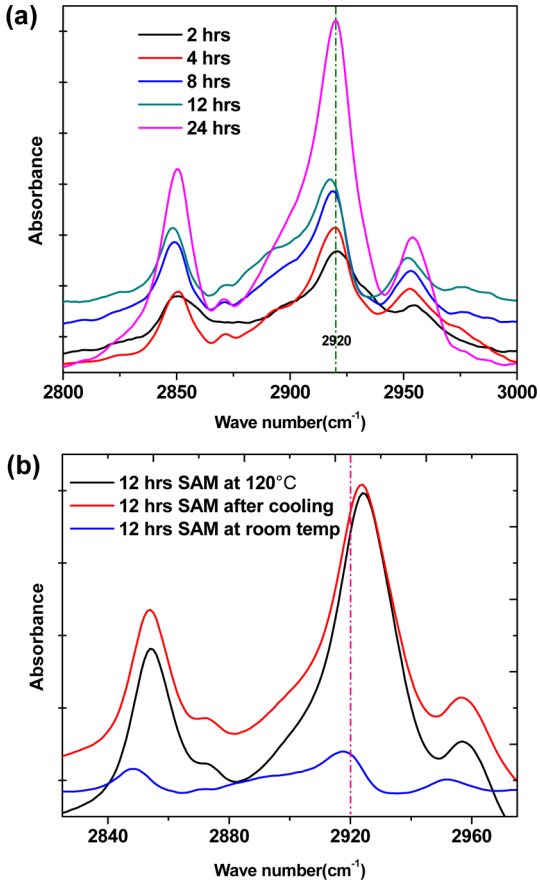

Figure 1. (a) IRRAS of SAM generated at different dipping time (solution pH = 7, temperature =297 K). (b) IRRAS showing the effect of temperature on the stability of SAM (Dipping time 12 h, pH = 7).

Figure 1a represents FTIR spectra of sodium oleate monolayer self assembled on a steel surface with different dipping times from 2−24 h at pH 7. Generally during formation of SAM three main steps were reported. The first one is the fastest step where the head group of the surfactant molecule from solution adsorbs on the substrate. The second step is the straightening or standing up of the hydrocarbon chains takes place; this phase is slower than the first step. In the last stage reorientation of the molecule takes place; it will take a time interlude of minutes to several hours depending on adsorbate. Again, this step is slower than first two stages. Here each step requires its own time scale; they show a characteristic signature in the vibration spectra. There is an increase in the integrated intensity that parallels the blue shift in the CH_2 stretch.[3,32] In the present case as time increases, the intensity of the peaks were also increased along with a blue shift in the CH_2 stretch from 2920.86 to 2917.59 cm^{-1}. At 12 h we have observed highest blue shift in the CH_2 stretch, so this time period was optimized for further experiments.

The band width of the peaks is useful in determining the order and packing of the aliphatic chains in the monolayer. The

full width at half-maximum (FWHM) of the asymmetric CH_2 stretch is a measure of the conformational order of alkyl chains in the SAM film.[33] FWHM for the asymmetric CH_2 stretch at 2, 4, 8, 12, and 24 h are found to be 19.9, 19.6, 18.6, 16.3, and 18.4 cm^{-1}, respectively. Among all these spectra, the SAM generated at 12 h which had the asymmetric CH_2 stretch at 2917.59 cm^{-1} and FWHM 16.3 cm^{-1} indicates the formation of a well organized close packed monolayer. For loosely packed SAM, FWHM asymmetric CH_2 stretch is >18 cm^{-1} and a randomly oriented film gives FWHM greater than 35 cm^{-1}.[34]

Figure 1B represents the temperature dependence of the peak frequency of the asymmetric CH_2 stretch in sodium oleate monolayer on a steel surface. The frequency of the peak increases from 2917 to 2924 cm^{-1} for the temperature range from 24−120 °C. The band width also increases sharply up to a value of 20.1 cm^{-1} at 120 °C. The reason for the variation in intensity of the asymmetric CH_2 stretch is due to Gauche defect and untilting. Here the intensity increases with temperature which can be attributed to Gauche defect generation.[33,35] With increasing temperature gauche defects were accumulated thus reducing the order in the monolayer.[32,36] Peak frequency and intensity value does not return to their original values on cooling by which we infer the creation of disorder into the SAM by the heat treatment.

Contact Angle Measurements. Table 1 shows the contact angle of water on sodium oleate self assembled monolayer as a function of dipping time. As dipping time increases the contact angle also increases. Contact angle of water (θ_{water}) on sodium oleate SAM generated at 12 h is 113° (at room temperature) which indicates the hydrophobic nature of the surface. This is because the polar head group of sodium oleate is fixed to the surface and the non polar tail group is projected towards the space and is normal to the surface. So there is less interaction between non polar tail groups of sodium oleate adsorbed on the surface and water; therefore water beads up instead of spreading. Increasing time of exposure in solution from 2−12 h leads to the gradual increase in contact angle from 88−113°. This indicates that the sodium oleate SAM is conformationally ordered at 12 h. A comparatively low contact angle below 100° was observed for the SAM generated at less than 12 h. This reveals disorder in the SAM.[33,37] This can also be confirmed by looking at the antisymmetric methylene stretching frequency which varies from 2920.86−2917.59 cm^{-1}. A decrease in contact for the sample after cooling from 120 °C was observed because of the defect created on the SAM after heat treatment.

Table 1. IRRAS and Contact Angle Measurement for SAM Characterization

dipping time (h)	C−H stretch (cm^{-1})	FWHM	contact angle
SAM Generated at Different Times at pH 7			
2	2920.86	19.9	88.84 ± 2
4	2920.04	19.6	98.30 ± 1
8	2919.36	18.6	100.27 ± 2
12	2917.59	16.3	113.02 ± 1
24	2919.95	18.4	102.01± 2
Effect of Temperature on the Stability of SAM Generated at 12 h at pH 7			
at 120 °C	2924	20.1	
after cooling	2923	19.7	98.86± 2

Electrochemical Measurements. *OCP Measurements.* Using a reference electrode, the potential between the electrode surface and the electrolyte interface can be measured. There is a formation of equilibrium between the interface, and the equilibrium deviates if there is any change in the interface or because of some reactions on the electrode surface. The equilibrium potential in the open circuit, that is, with no electrical interruption or without applying any external load, is normally termed as open circuit potential (OCP) or steady state potential. Normally OCP is considered as a measure of nobleness of the electrode surface.[38]

The OCPs and corrosion measurement of the specimens were carried out by immersing test samples in different types of electrolytes. The first set of experiments were carried out using SAM covered samples (using sodium oleate solution of different pH for 12 h) in 3.5 wt % NaCl solution with respect to the Ag/AgCl electrode. The second and third sets of experiments were carried out by using bare steel as sample and solution with and without sodium oleate at different pH as electrolyte.

Figure 2a shows the change in potential as a function of immersion time (400 s) in 3.5% NaCl solution for bare steel and SAM (by using pH 2.5, 7, and 9 sodium oleate solution) generated on steel at room temperature for 12 h. Compared to bare steel, the potential of the SAM covered sample shifts towards a more positive direction with time. For SAM covered steel at different pH, the negative potential stands in the order pH 2.5 < pH 9 < pH 7. From this result, we can conclude that the Sodium Oleate SAM covered sample generated for 12 h in acidic pH is more resistant to degradation.

Figures 2b and 2c show the OCP of the bare steel samples immersed in solution without and with sodium oleate at various pH. Without sodium oleate the bare steel samples show more negative open circuit potential at pH 2.5; this is due to the formation of soluble corrosive product and lack of formation of the passive film on the substrate surface. In the presence of sodium oleate, the bare steel shows a more positive potential by adsorbtion on the surface of the substrate that it helps to slow the degradation of the material.

Polarization Measurements. The polarization behavior of bare steel and SAM (12 h by using pH 2.5, pH 7, and pH 9 H_2O) covered steel in 3.5% NaCl solution at room temperature was measured and shown in Figure 3a. Electrochemical parameters like corrosion potential (E_{corr}), corrosion current density (I_{corr}), cathodic Tafel Slope (β_c), anodic Tafel Slope (β_a), were calculated. I_{corr} of SAM covered steel decreases compared to bare steel, I_{corr} stands in the order pH 2.5 < pH 9 < pH 7 for the SAM covered samples generated at different pHs.

Figure 3b shows Tafel measurements for bare steel immersed in aqueous media having different pHs without sodium oleate. The E_{corr} value was shifted towards more positive potential in the order pH 2.5 < pH 7 < pH 9. This is because in acidic medium, ferrous oxide (FeO) is soluble and dissolves as it is formed so that the fresh surface is available for corrosion. The corrosion reaction takes place at a greater rate in the paucity of the protective oxide film as the metal surface is in direct contact with the acid solution. At pH 7, the rate at which oxygen reacts with absorbed atomic hydrogen directs largely the corrosion rate by depolarizing the surface and permitting the reduction reaction to persist. At pH 9, formation of the additional protective Fe_2O_3 takes place because of an increase in the rate of the reaction of oxygen with $Fe(OH)_2$ (hydrated FeO) in the oxide layer; consequently the corrosion rate decreases.[39]

Figure 3c shows Tafel measurements for bare steel immersed in sodium oleate solution having different pH. E_{corr} value was

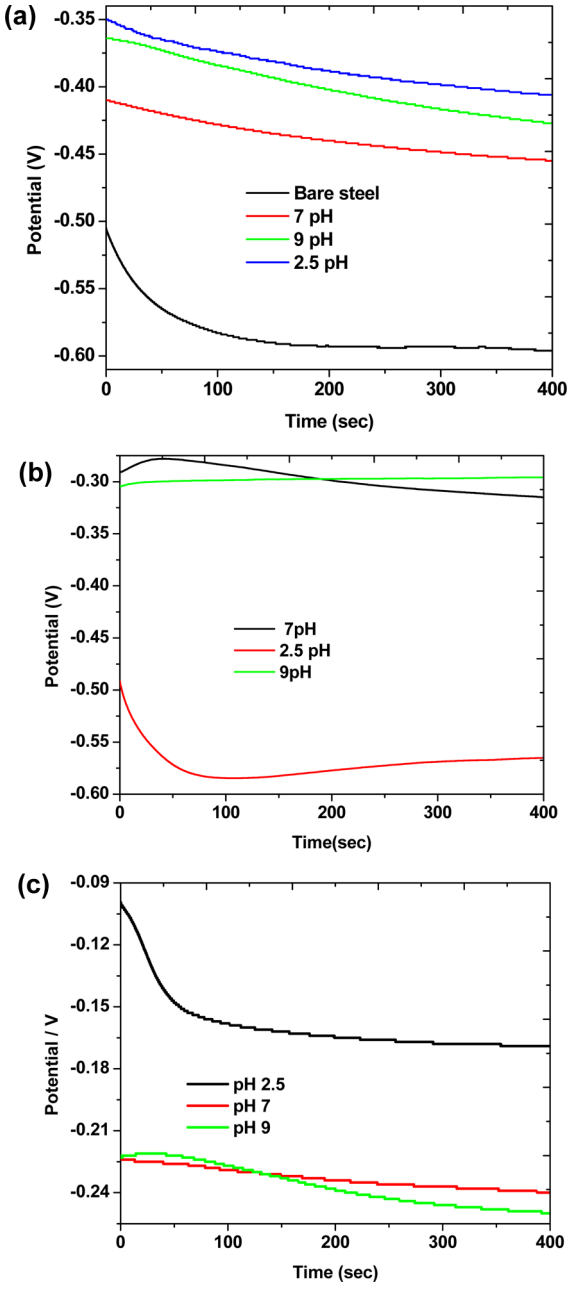

Figure 2. (a) OCP measurement for the SAM (generated for 12 h at different pH) in 3.5% NaCl. OCP measurement for bare steel immersed in aqueous solution (b) without sodium oleate and (c) with sodium oleate at different pHs.

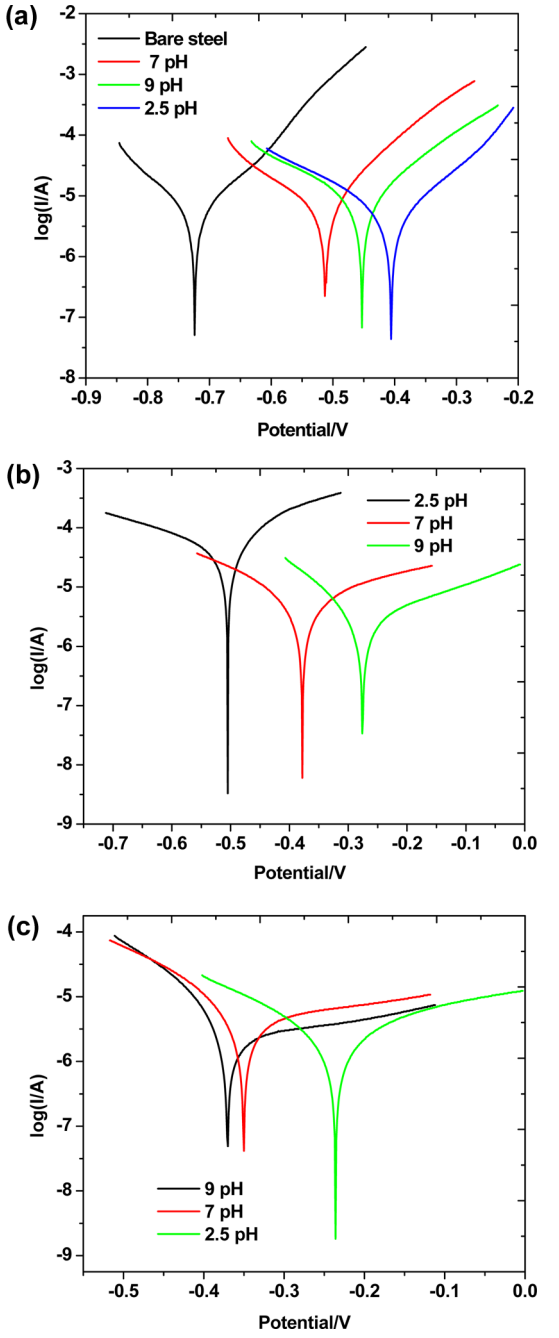

Figure 3. (a) Tafel measurement of the SAM generated steel (for 12 h at different pH) in 3.5% NaCl solution. Tafel measurement for bare steel immersed in aqueous solution (b) without sodium oleate and (c) with sodium oleate at different pHs.

shifted towards more positive potential in the order pH 9 < pH 7 < pH 2.5. The isoelectric point of steel has been projected to be between pH 5.2 to 6.7; this suggests that below this pH range the metal surface acquires a positive charge.[9] Therefore negatively charged sodium oleate binds to the steel surface through the electrostatic attraction and forms a protective layer to reduce the corrosion rate. It has been reported that colloid precipitates of oleic acid are charged positively when the pH of the solution is less than 3.5.[28] Since the steel surface also was charged positively, it was doubtful that the colloids would adsorb on the steel surface directly through electrostatic attraction. At the primary stage, the oleic acids might have adsorbed on the iron surface chemically and then, the colloids may possibly have adsorbed on the chemisorbed surface through van der Waals forces. A summary of corrosion data from Tafel measurements is presented in Table 2.

Electrochemical Impedance Spectroscopy (EIS) Measurements. Electrochemical impedance spectroscopy is one of the most helpful and revealing method for the corrosion measurement of coated metals. They are appropriate for in situ and non-destructively probing relaxation phenomena over a wide frequency range.[40] From this, we can acquire, validate, and quantitatively interpret the experimental impedances. In the present work, the impedance measurements were carried at open circuit potential in the frequency range 100 kHz to 10 mHz.

dx.doi.org/10.1021/am4028857 | ACS Appl. Mater. Interfaces 2013, 5, 10738−10744

Table 2. Corrosion Data Obtained from Tafel Measurements[a]

sample	E_{corr} (mV)	I_{corr} (μA cm^{-2})	β_c (1/V)	β_a (1/V)	corrosion rate (miles/year)
SAM Generated for 12 h at Different pH (Electrolyte 3.5% NaCl)					
bare steel	−0.724	6.025	9.936	9.019	5.508
pH 7	−0.513	5.845	7.686	12.889	5.344
pH 2.5	−0.406	3.820	10.430	8.347	3.495
pH 9	−0.495	5.227	9.208	9.027	4.779
Bare Steel Immersed in Aqueous Media Having Distinct pH without Sodium Oleate					
pH 7	−0.378	5.982	5.823	4.130	5.469
pH 2.5	−0.505	12.64	30.79	16.80	11.55
pH 9	−0.276	3.376	8.038	3.839	3.086
Bare Steel Immersed in Aqueous Media Having Distinct pH with Sodium Oleate					
pH 7	−0.350	4.563	11.09	2.627	4.171
pH 2.5	−0.236	2.554	6.621	4.459	2.335
pH 9	−0.370	5.115	8.096	1.637	4.676

[a]Figures 3a−3c.

The measured impedance data were given as typical Nyquist plots. Complex plane (Nyquist) plots are often used in the electrochemical literature because they allow for an easy calculation of the impedance corrosion elements. In general, in the Nyquist diagram, the interception of the real axis at the higher frequency is associated to the electrolyte resistance (R_s) and that which intercepts at the lower frequency is attributed to the charge transfer resistance (R_{ct}) and the degree of corrosion resistance can be measured as the area enclosed by the loop. Impedance spectra with the fitted electrical equivalent circuit (EEC) facilitate understanding the electrochemical process taking place at the surface. So to acquire impedance parameters, the experimentally determined EIS data were fitted with a appropriate equivalent circuit (which possesses a lesser percentage of error), with the aid of the ZSimpWin 3.21 software. To obtain exact fitting results, the capacitance elements (C) in the employed EEC are all replaced by constant phase elements (CPE). The impedance of CPE is defined by the following equation:

$$Z(j\omega) = (Q)^{-1}(j\omega)^{-n}$$

Where Q is the CPE constant, j is the imaginary unit, ω the angular frequency ($\omega = 2\pi f$, f is the frequency), and n the CPE exponent ($-1 \leq n \leq 1$). CPE describes an ideal capacitor for $n = 1$, an ideal inductor for $n = -1$, and an ideal resistor for $n = 0$, and if there is a decrease in the n value this means that the non-uniform distribution of current arises from surface roughness and surface defects.[41−43]

The EEC given in Figure 4 was used to fit measured impedance data in all the cases. This equivalent model can be represented as $R_s(Q_{coat}(R_{coat}\ (Q_{dl}R_{ct})))$, where R_s is the solution resistance, Q_{coat} is the constant phase element (CPE) of the film, R_{coat} the resistance of the film, Q_{dl} the CPE of the double layer, and R_{ct} the resistance of the double layer.

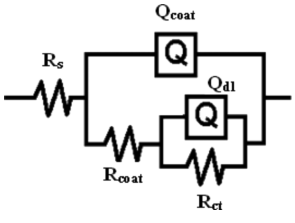

Figure 4. Electrical equivalent circuit (EEC).

In the discussion part the constant phase element is referred as capacitance element because in all the cases the constant phase element coefficient is nearly equal to 1, that is, $n \approx 1$; hence $Q \approx C$.

Figure 5a shows typical Nyquist impedance plot for the corrosion behavior of bare steel and SAM (generated for 12 h by using pH 2.5, pH 7, and pH 9 solution) on steel in 3.5% NaCl solution at room temperature.

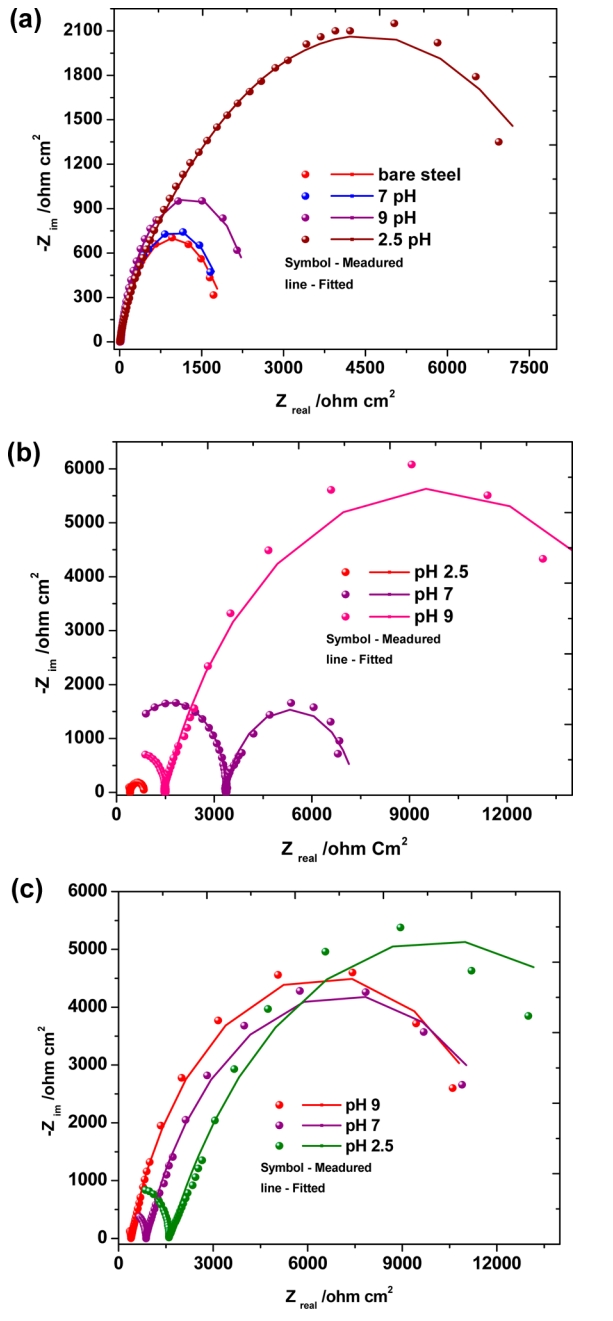

Figure 5. (a) EIS measurement of the SAM generated steel (for 12 h at different pH) in 3.5% NaCl solution. EIS measurement for bare steel immersed in aqueous solution (b) without sodium oleate and (c) with sodium oleate at different pHs.

dx.doi.org/10.1021/am4028857 | ACS Appl. Mater. Interfaces 2013, 5, 10738−10744

Table 3. Corrosion Data Obtained from EIS Technique[a]

sample	Q_{coat} ($\mu\Omega^{-1}$ cm^{-2} S^{-1})	n	R_{coat} (Ω cm^2)	Q_{dl} ($\mu\Omega^{-1}$ cm^{-2} S^{-1})	n	R_{ct} (Ω cm^2)	% error
SAM Generated for 12 h at Different pH (Electrolyte 3.5% NaCl)							
bare steel	228.4	0.867	14.1	256.6	0.735	1636	4.438
pH 7	7.49	0.826	3.225	157.5	0.802	1657	1.552
pH 2.5	14.65	0.800	966	37.97	0.800	5974	3.733
pH 9	4.33	0.833	4.187	128	0.837	2146	1.975
Bare Steel Immersed in Aqueous Media Having Distinct pH without Sodium Oleate							
pH 7	8.099×10^{-4}	1	3332	236	0.8325	3468	1.576
pH 2.5	9.706×10^{-4}	1	416.3	81.91	0.8943	421.7	1.414
pH 9	9.530×10^{-4}	1	1443	141	0.7645	11657	3.367
Bare Steel Immersed in Aqueous Media Having Distinct pH with Sodium Oleate							
pH 7	0.1066	1	869.2	152.5	0.7518	10030.8	2.227
pH 2.5	9.505×10^{-4}	1	1613	15.75	0.6908	11387	2.826
pH 9	148.6	1	396.9	159.8	0.8013	10203.1	2.098

[a]Figures 5a–5c.

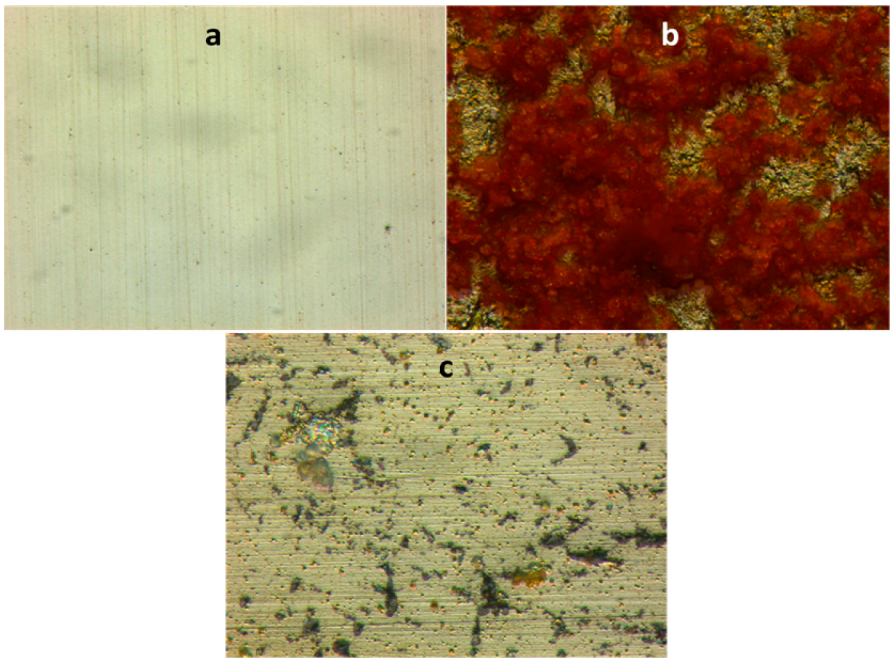

Figure 6. 3D optical profilometer images. (a) Bare steel. (b) Bare steel immersed in pH 2.5 aqueous solution for 24 h. (c) Bare steel immersed in pH 2.5 sodium oleate solution for 24 h.

The corrosion parameters calculated from the EIS (EEC fitted) are tabulated in Table 3. All the curves from Figure 5a appear to be similar with respect to their shape, but they vary significantly in their size. This reveals that the same fundamental course of action must be happening on all these coatings but over a different effective area in each case. Each curve consists of two semicircles each at the higher- and the lower-frequency end, indicating two relaxation processes in the mechanism involved. SAM generated at pH 2.5 for 12 h were found to exhibit Nyquist loops with distended area with higher-charge transfer resistance and minimum double layer capacitance revealing increased corrosion resistance followed by SAM generated at pH 9 and 7 for 12 h.

Figure 5b and 5c represents the corrosion inhibition of the steel by sodium oleate molecule at different pH in aqueous environment. At acidic pH the adsorbed colloidal precipitates of oleic acid on the steel surface through electrostatic attraction acts as a passive layer or barrier in the interface between substrate and electroactive media. This reduces the contact between the steel surface and the corrosive media. As a result, the maximum coating resistance (R_{coat}) with minimum coating capacitance (Q_{coat}) was observed. The dielectric behavior of the SAM decreased the double layer capacitance and offered more resistance for charge transfer.

Surface Morphology. To establish the corrosion inhibition of the sodium oleate molecule at pH 2.5, 3D profilometer was used to take the true color image. In Figure 6, (a) presents the bare steel surface after polishing (before exposure to corrosive environment); (b) steel immersed in pH 2.5 solution without sodium oleate for about 24 h; and (c) steel immersed in pH 2.5 solution with 1 mM sodium oleate for about 24 h. In the absence of sodium oleate the steel sample degraded significantly and formation of rust can be seen. However, in the presence of sodium oleate, the rate of rust formation diminished and the steel sample is not degraded as much. Here the adsorbed sodium oleate performs as a barrier film and protects steel from corrosion.

4. CONCLUSION

Sodium oleate monolayer was successfully generated on a mild steel surface. The contact angle and IR data indicate the formation of a highly ordered monolayer at about 12 h. The monolayer at this time shows highest contact angle with strong hydrophobic nature. The SAM treated at higher temperature shows defects because of reorientation of molecules on the substrate. Electrochemical measurements of the SAM covered steel surface showed the anticorrosive character. The sodium oleate acts as a corrosion inhibitor for steel in acidic pH by forming a barrier to interface between substrate and electroactive media.

AUTHOR INFORMATION

Corresponding Author

*E-mail: drtvvenkatesha@yahoo.co.uk (T.V.V.). Phone: +91-9448855079. Fax: +91-08282-256255

Notes

The authors declare no competing financial interest.

ACKNOWLEDGMENTS

The authors are grateful to Department of Chemistry, Kuvempu University, and Mechanical Engineering Department, Indian Institute of Science Bangalore, Karnataka, India, for providing lab facilities. We acknowledge the help given by Mr. H. S. Shamasundar, Mr. S. Ranganatha, Mr. Sudheendra Shastri, Mr. G. Chidananda, and Mr. M. Praveena in conducting different experiments.

REFERENCES

(1) Gooding, J. J.; Mearns, F.; Yang, W.; Liu, J. *Electroanal.* **2003**, *15*, 81−96.
(2) Li, Y.; Huang, J.; Mclver, R. T., Jr.; Hemminger, J. C. *J. Am. Chem. Soc.* **1992**, *114*, 2428−2432.
(3) Schreiber, F. *Prog. Surf. Sci.* **2000**, *65*, 151−256.
(4) Kotz, J.; Kosmella, S.; Beitz, T. *Prog. Polym. Sci.* **2001**, *26*, 1199−1232.
(5) Rosei, F.; Schunack, M.; Naitoh, Y.; Jiang, P.; Gourdon, A.; Laegsgaard, E.; Stensgaard, I.; Joachim, C.; Besenbacher, F. *Prog. Surf. Sci.* **2003**, *71*, 95−146.
(6) Delamarche, E.; Michel, B.; Kang, H.; Gerber, C. *Langmuir* **1994**, *10*, 4103−4108.
(7) Rozeenfel, I. L.; Loskutov, A. I.; Alekseev, V. N. *Inst. Phys. Chem.* **1982**, *2*, 233−237.
(8) Hautman, J.; Klein, M. L. *Phys. Rev. Lett.* **1991**, *67*, 1763−1766.
(9) Kanagalasara, V.; Saxena, D.; Biswas, S. K. *J. Phys. Chem. C* **2012**, *116*, 20830−20838.
(10) Sheen, C. W.; Shi, J. X.; Maartensson, J.; Parikh, A. N.; Allara, D. L. *J. Am. Chem. Soc.* **1992**, *114*, 1514−1515.
(11) Caprioli, F.; Decker, F.; Marrani, A. G.; Beccari, M.; Castro, V. D. *Phys. Chem. Chem. Phys.* **2010**, *12*, 9230−9238.
(12) Rivas, M. V.; Mendez De Leo, L. P.; Hamer, M.; Carballo, R.; Williams, F. J. *Langmuir* **2011**, *27*, 10714−10721.
(13) Schonherr, H.; Ringsdorf, H. *Langmuir* **1996**, *12*, 3891−3897.
(14) Kluth, G. J.; Sung, M. M.; Maboudian, R. *Langmuir* **1997**, *13*, 3775−3780.
(15) Yun, D. J.; Rhee, S. W. *J. Electrochem. Soc.* **2008**, *155*, H357−H362.
(16) Allara, D. L.; Nuzzo, R. G. *Langmuir* **1985**, *1*, 45−52.
(17) Risse, T.; Hill, T.; Schmidt, J.; Abend, G.; Hamann, H.; Freund, H. J. *J. Phys. Chem. B* **1998**, *102*, 2668−2676.
(18) Raman, A.; Dubey, M.; Gouzman, I.; Gawalt, E. S. *Langmuir* **2006**, *22*, 6469−6472.
(19) Gao, W.; Dickinson, L.; Grozinger, C.; Morin, F. G.; Reven, L. *Langmuir* **1996**, *12*, 6429−6435.
(20) Ye, S.; Li, G.; Noda, H.; Uosaki, K.; Osawa, M. *Surf. Sci.* **2003**, *529*, 163−170.
(21) Bain, C. D.; Troughton, E. B.; Tao, Y. T.; Evall, J.; Whitesides, G. M.; Nuzzo, R. G. *J. Am. Chem. Soc.* **1989**, *111*, 321−335.
(22) Hamoudi, H.; Prato, M.; Dablemont, C.; Cavalleri, O.; Canepa, M.; Esaulov, V. A. *Langmuir* **2010**, *26*, 7242−7247.
(23) Porter, M. D.; Bright, T. B.; Allara, D. L.; Chidsey, C. E. D. *J. Am. Chem. Soc.* **1987**, *109*, 3559−3568.
(24) Keller, C. A.; Kasemo, B. *Biophys. J.* **1998**, *75*, 1397−1402.
(25) Maeda, Y.; Yamamoto, H.; Kitano, H. *J. Phys. Chem.* **1995**, *99*, 4837−4841.
(26) Caldwell, W. B.; Campbell, D. J.; Chen, K.; Herr, B. R.; Mirkin, C. A.; Malik, A.; Durbin, M. K.; Dutta, P.; Huang, K.G. *J. Am. Chem. Soc.* **1995**, *117*, 6071−6082.
(27) Ogawa, S.; Fan, F. F.; Bard, A. J. *J. Phys. Chem.* **1995**, *99*, 11182−11189.
(28) Luo, H.; Guan, Y. C.; Han, K. N. *Corros. Sci.* **1998**, *54*, 619−627.
(29) Xu, X.; Yu, Z.; Zhu, Y.; Wang, B. *Diamond Relat. Mater.* **2005**, *14*, 206−212.
(30) Kumar, D.; Biswas, S. K. *Colloids Surf., A* **2010**, *356*, 112−119.
(31) Mccafferty, E. *Corros. Sci.* **2005**, *47*, 3202−3215.
(32) Vericat, C.; Vela, M. E.; Benitez, G.; Carro, P.; Salvarezza, R. C. *Chem. Soc. Rev.* **2010**, *39*, 1805−1834.
(33) Khatri, O. P.; Bain, C. D.; Biswas, S. K. *J .Phys. Chem. B* **2005**, *109*, 23405−23414.
(34) Seip, C. T.; Granroth, G. E.; Meisel, M. W.; Talham, D. R. *J. Am. Chem. Soc.* **1997**, *119*, 7084−7094.
(35) Prathima, N.; Harini, M.; Rai, N.; Chadrashekara, R. H.; Ayappa, K. G.; Sampath, S.; Biswas, S. K. *Langmuir* **2005**, *21*, 2364−2374.
(36) Khatri, O. P.; Biswas, S. K. *Surf. Sci.* **2006**, *600*, 4399−4404.
(37) Petrovíc, Z.; Hukovíc, M. M.; Babíc, R. *Prog. Org. Coat.* **2008**, *61*, 1−6.
(38) Kanagalasara, V.; Venkatarangaiah, V. T. *Appl. Surf. Sci.* **2011**, *257*, 8929−8936.
(39) *DOE Fundamentals Handbook Chemistry*; U.S. Department of Energy: Washington, D.C., 1993; CH02−15.
(40) Hu, J. M.; Liu, X. L.; Zhang, J. Q.; Cao, C. N. *Prog. Org. Coat.* **2006**, *55*, 388−392.
(41) Punith Kumar, M. K.; Venkatarangaiah, V. T.; Pavitra, M. K.; Nithyananda Shetty, A. *Synth. React. Inorg., Met.-Org., Nano-Met. Chem.* **2012**, *42*, 1426−1434.
(42) Mishra, A. K.; Balasubramaniam, R.; Tiwari, S. *Anti-Corros. Methods Mater.* **2007**, *54*, 37−46.
(43) Punith Kumar, M. K.; Venkatarangaiah, V. T.; Pavitra, M. K.; Nithyananda Shetty, A. *Phys. Scr.* **2011**, *84*, 1−10.